Supplementary Data

p53 maintains baseline expression of multiple tumor suppressor genes

Authors: Kyrie Pappas[1,2,3], Jia Xu[1,2§], Sakellarios Zairis[4§], Lois Resnick-Silverman[1,2], Francesco Abate[4,5], Nicole Steinbach[1,2,6], Sait Ozturk[1,2], Lao H. Saal[7,8,9], Tao Su[10], Pamela Cheung[1,2], Hank Schmidt[2,11,12], Stuart Aaronson[1,2], Hanina Hibshoosh[10], James Manfredi[1,2‡], Raul Rabadan[4,5‡], Ramon Parsons[1,2,*]

Correspondence to: ramon.parsons@mssm.edu

This PDF file includes:

Supplementary Figures S1-S10

Supplementary Tables S1-S3

Captions for Supplementary Spreadsheets S1-S5
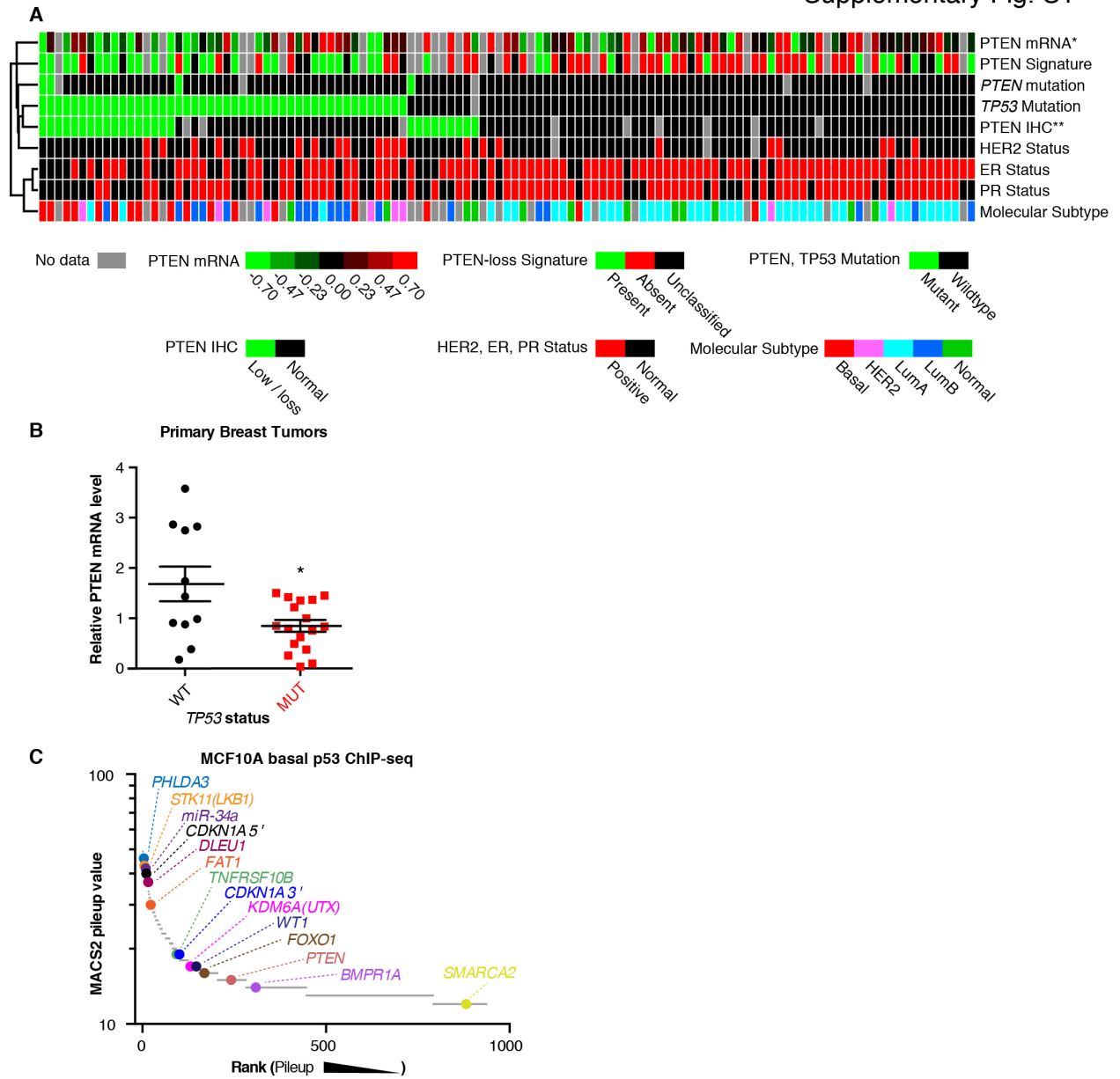
Supplementary Materials and Methods

Supplementary References

Other Supporting Information for this manuscript includes the following:

Supplementary Spreadsheets S1-S5 (separate Excel files)

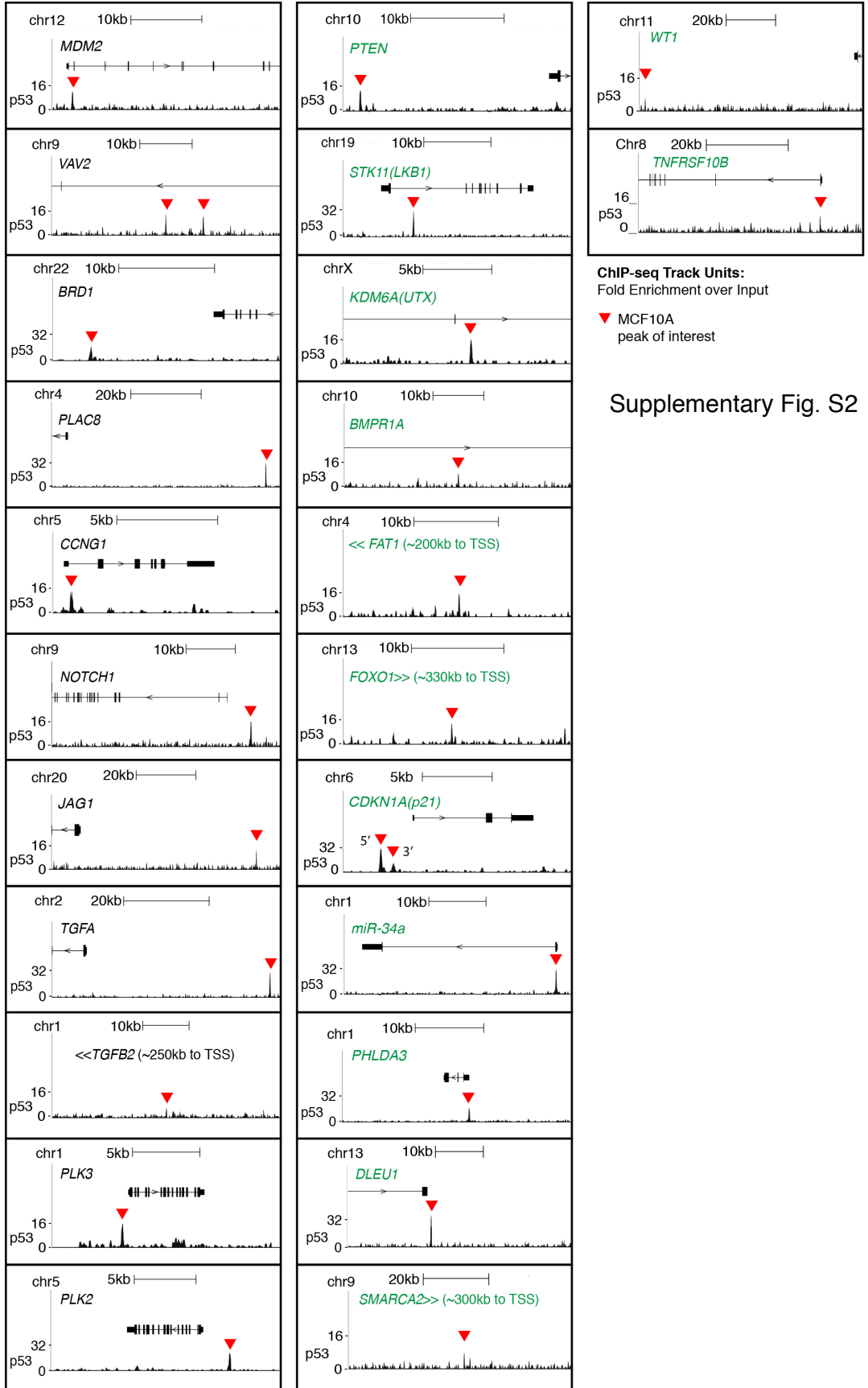**Supplementary Figures S1-S10:**

Supplementary Fig. S1

A

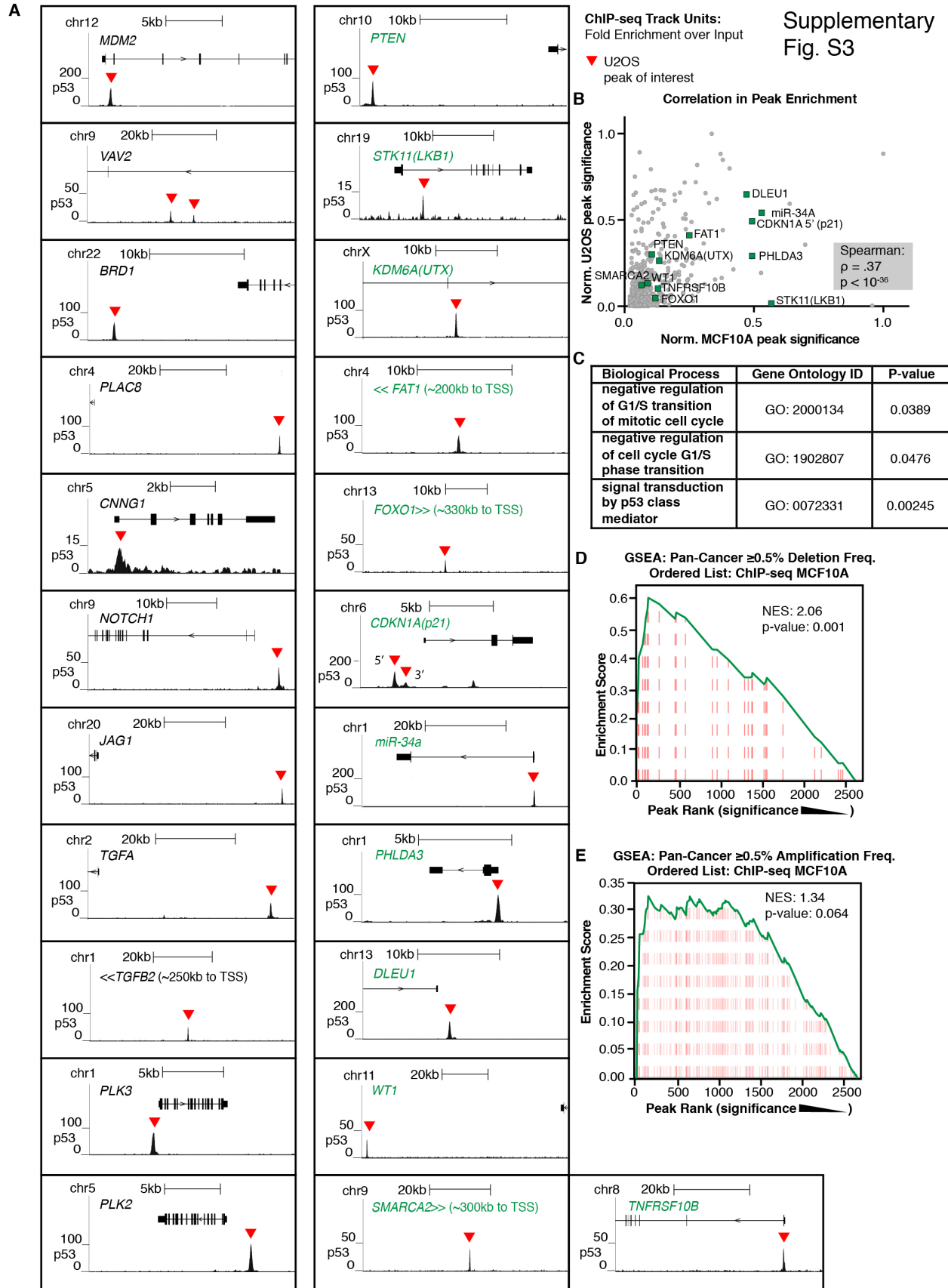**B** Primary Breast Tumors

C MCF10A basal p53 ChIP-seq

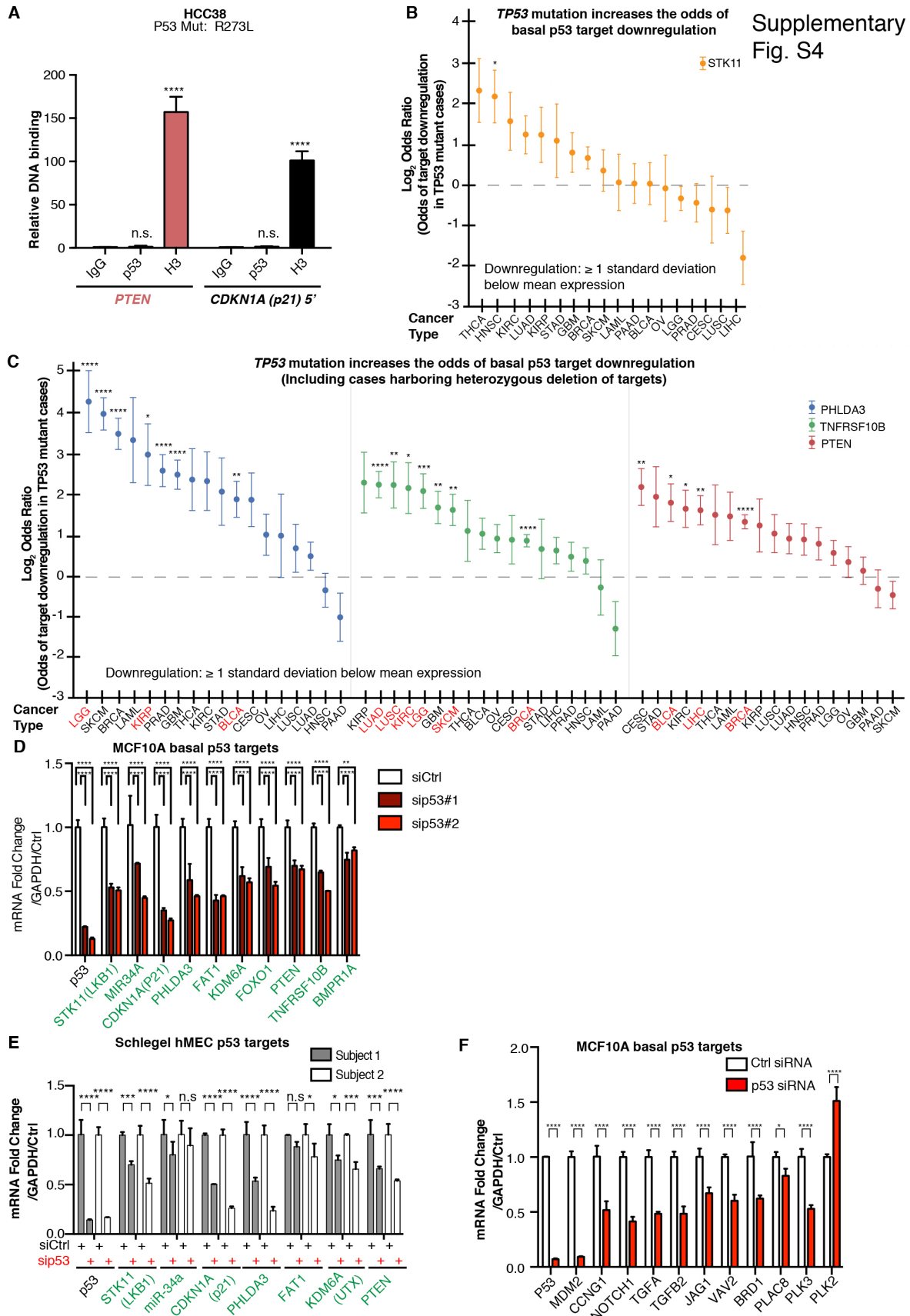**Supplementary Fig. S1: Basally expressed p53 may have important tumor suppressor targets. (A)** Primary breast tumors were measured and analyzed for several parameters (from top to bottom): PTEN mRNA by microarray (*p≤.05, n=95 by Mann Whitney test, expression lower in *TP53*-mutant group), *PTEN* signature (51), *PTEN* mutation, *TP53* mutation, PTEN IHC status (**p≤.01, n=107 by Chi-squared test, expression is lower in *TP53*-mutant group), Her2- ER- PR- status, and molecular subtype. Color key is indicated**. (B)** PTEN transcript measured by qRT-PCR in primary breast tumors (from the same cohort as above) that were either wild-type (WT, n=11) or mutant (MUT, n=18) for *TP53*. Numbers expressed as a fold change from MCF10A cells, normalized to GAPDH. Error bars: mean ± s.e.m. Measurements made in triplicate. Significance: Mann-Whitney test. (*p≤.05) **(C)** The top 1000 MCF10A basal p53 ChIP-seq peaks were ranked based on MACS2 read pileup value at peak summit. The top 63 peaks were artifacts and were removed. Tumor suppressor targets of basal p53 are indicated.

Supplementary Fig. S2

ChIP-seq Track Units:
Fold Enrichment over Input

▼ MCF10A
peak of interest

Supplementary Fig. S2: Binding targets of basal p53 in MCF10A cells. ChIP-seq was performed for basal p53 in MCF10A cells, tracks show fold enrichment over input for genes of interest. Location of peak is indicated by red triangle. Tumor suppressor targets are shown in green, other targets in black.

A

Supplementary Fig. S3

ChIP-seq Track Units:
Fold Enrichment over Input

▼ U2OS peak of interest

B Correlation in Peak Enrichment

Spearman:
ρ = .37
p < 10⁻³⁶

C

Biological Process	Gene Ontology ID	P-value
negative regulation of G1/S transition of mitotic cell cycle	GO: 2000134	0.0389
negative regulation of cell cycle G1/S phase transition	GO: 1902807	0.0476
signal transduction by p53 class mediator	GO: 0072331	0.00245

D GSEA: Pan-Cancer ≥0.5% Deletion Freq.
Ordered List: ChIP-seq MCF10A

NES: 2.06
p-value: 0.001

E GSEA: Pan-Cancer ≥0.5% Amplification Freq.
Ordered List: ChIP-seq MCF10A

NES: 1.34
p-value: 0.064

Supplementary Fig. S3: Exploring the binding targets of basal p53. (A) Previously published ChIP-seq data for basal p53 in U2OS cells (DMSO-treated) (52) was analyzed, tracks show fold enrichment over input for genes of interest. Location of peak is indicated by red arrow. Tumor suppressor targets are shown in green, other targets in black. **(B)** Plot of normalized significance of U2OS versus MCF10A basal p53 ChIP-seq peaks. ρ refers to the Spearman correlation coefficient comparing the two lists, and the corresponding p-value is reported. **(C)** Gene Ontology (GO) for biological processes was performed on the top 200 genes of the MCF10A basal p53 ChIP-seq list using the PANTHER Overrepresentation Test (release 20160715) with the Bonferroni correction. GO ID and p-values are indicated. **(D)** GSEA of basal MCF10A p53 ChIP-seq list (ordered by significance) for genes deleted, and **(E)** for genes amplified in ≥0.5% of all cancers in TCGA. Enrichment scores and p-values are indicated.
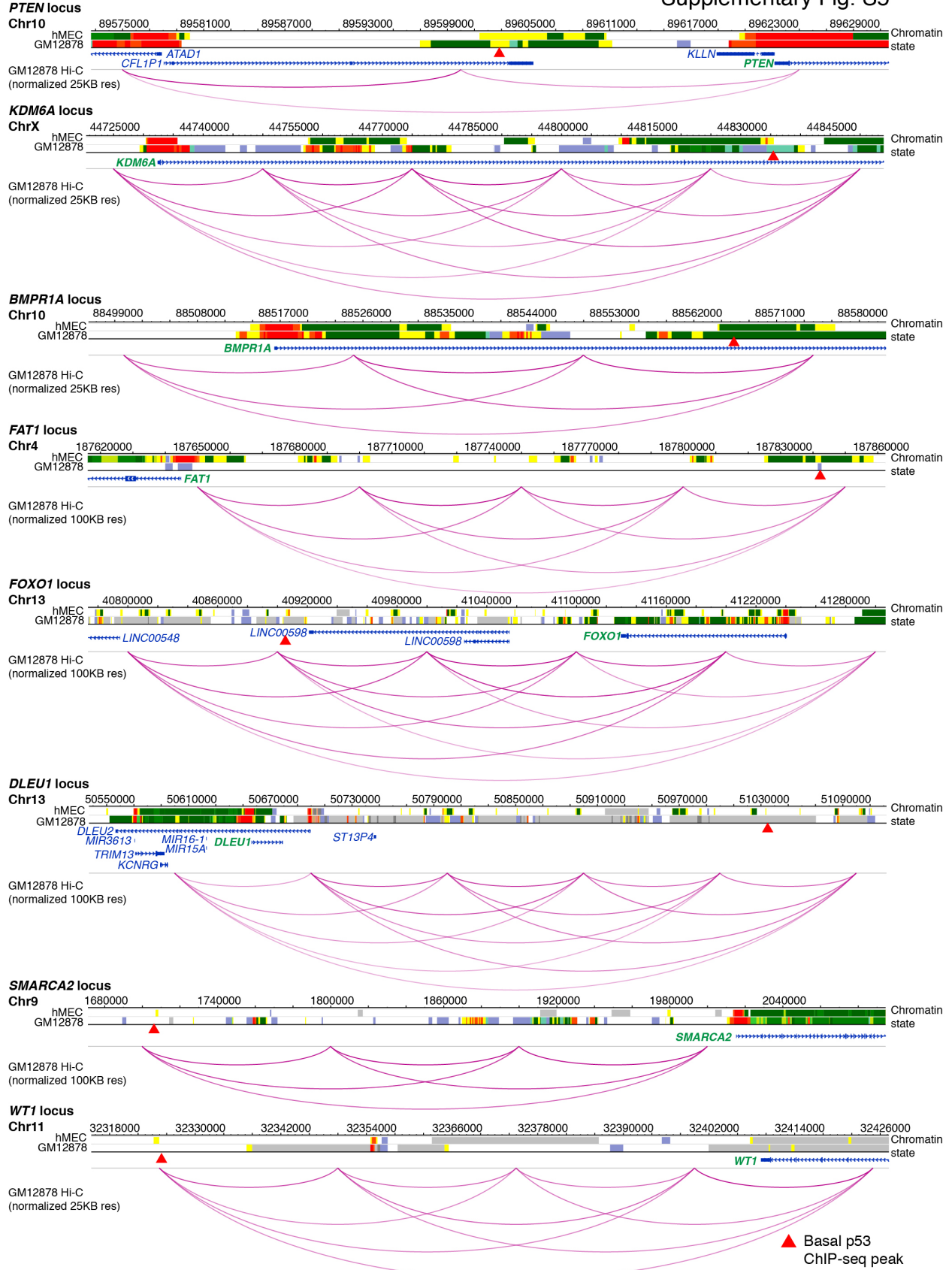
A HCC38 — P53 Mut: R273L — Relative DNA binding; conditions IgG, p53, H3 for PTEN and CDKN1A (p21) 5′

B *TP53* mutation increases the odds of basal p53 target downregulation — Log$_2$ Odds Ratio (Odds of target downregulation in TP53 mutant cases); STK11; Downregulation: ≥ 1 standard deviation below mean expression — Supplementary Fig. S4

C *TP53* mutation increases the odds of basal p53 target downregulation (Including cases harboring heterozygous deletion of targets) — Log$_2$ Odds Ratio (Odds of target downregulation in TP53 mutant cases); PHLDA3, TNFRSF10B, PTEN; Downregulation: ≥ 1 standard deviation below mean expression

D MCF10A basal p53 targets — mRNA Fold Change /GAPDH/Ctrl; siCtrl, sip53#1, sip53#2; genes p53, STK11(LKB1), MIR34A, CDKN1A(P21), PHLDA3, FAT1, KDM6A, FOXO1, PTEN, TNFRSF10B, BMPR1A

E Schlegel hMEC p53 targets — mRNA Fold Change /GAPDH/Ctrl; Subject 1, Subject 2; siCtrl / sip53; genes p53, STK11 (LKB1), miR-34a, CDKN1A (p21), PHLDA3, FAT1, KDM6A (UTX), PTEN

F MCF10A basal p53 targets — mRNA Fold Change /GAPDH/Ctrl; Ctrl siRNA, p53 siRNA; genes P53, MDM2, CCNG1, NOTCH1, TGFA, TGFB2, JAG1, VAV2, BRD1, PLAC8, PLK3, PLK2

Supplementary Fig. S4: Wild-type p53 maintains expression of tumor suppressor target genes. (A) ChIP-qPCR in HCC38 cells (*TP53* Mut: R273L) for IgG (negative control), p53, and H3 (positive control) on *PTEN* and *5'CDKN1A*. Error bars: mean ± s.d. of representative experiment (performed twice), triplicate measurements. Significance (over IgG): two-way ANOVA, Dunnett's correction. TCGA data shows that *TP53* mutation **(B)** increases the relative risk for STK11 downregulation in some cancer types (defined as ≥ 1 s.d. below mean RNA-seq z-score), and **(C)** increases the relative risk for p53 target downregulation without correcting for copy number changes of the targets. Cancer types that increased at least one significance level (*) upon incorporation of deletions are written in red type. Error bars: $\log_2 OR$ ± s.d. of dataset. Acronyms for cancer types expanded in the Materials and Methods. Significance: Fisher's exact test. **(D)** MCF10A cells were transfected with control or p53-targeting siRNAs (individual siRNAs #1 and #2), qRT-PCR was used to measure transcript levels select basal p53 targets identified by ChIP-seq. Error bars: mean ± s.d., triplicate measurements. Significance: two-way ANOVA, Dunnet's correction. **(E)** Schlegel hMEC cells were transfected with control or p53-targeting siRNAs (pool of 4 siRNAs), qRT-PCR was used to measure transcript levels of select basal p53 targets identified by ChIP-seq in two tissue donors (Subjects 1 and 2). **(F)** MCF10A cells were transfected with control or p53-targeting siRNAs (pool of 4 siRNAs), qRT-PCR was used to measure transcript levels select basal p53 targets identified by ChIP-seq. Error bars: mean ± s.d., triplicate measurements. Significance: two-way ANOVA, Sidak's correction. (****$p \leq .0001$, ***$p \leq .001$, **$p \leq .01$, *$p \leq .05$, n.s. $p > .05$)

Supplementary Fig. S5
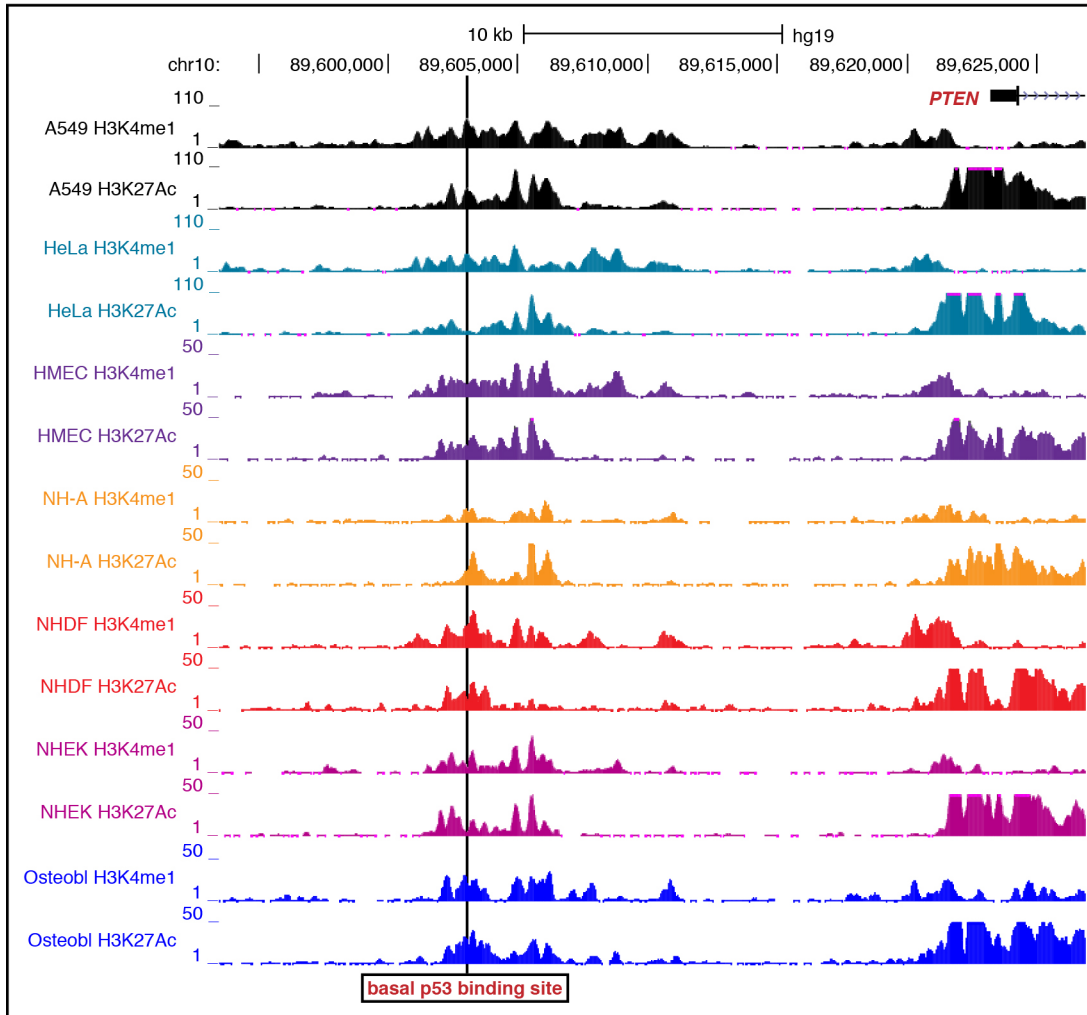
PTEN locus
Chr10

KDM6A locus
ChrX

BMPR1A locus
Chr10

FAT1 locus
Chr4

FOXO1 locus
Chr13

DLEU1 locus
Chr13

SMARCA2 locus
**Chr9**

WT1 locus
Chr11

▲ Basal p53
ChIP-seq peak

Supplementary Fig. S5: Long range chromatin interactions of enhancers with transcriptional start sites of basal p53 targets. Previously published Hi-C(53) and chromatin state (chromHMM) data(54) were adapted from the WashU genome browser(55,56) to investigate the physical interaction between select basal p53 binding sites (at least 20KB distal to the TSS) and the transcriptional start site (TSS) of putative target genes. Each target contains two chromatin state tracks (primary chromHMM from hMEC cells and GM12878 cells) and one normalized Hi-C track from GM12878 cells. See Materials and Methods for chromHMM color scheme. Resolution for Hi-C tracks is indicated for each target. Location of basal p53 peaks is denoted by the red triangle. Strength of Hi-C interaction is indicated by the hue of purple line (darker line = stronger interaction).

Supplementary Fig. S6: Enhancer for *PTEN* is present in multiple cell types. PTEN-eP53RE

is within a region of chromatin that interacts with H3K27Ac and H3K4me1 marks characteristic

of enhancers as measured by ChIP-seq enrichment in publicly available data from

Broad/ENCODE from multiple human cell types adapted from the UCSC genome browser

(54,57,58). PTEN-eP53RE is indicated by a black line through all data sets. A549: lung

adenocarcinoma cell line (black), HeLa: human cervical carcinoma cell line (light blue), HMEC:

human mammary epithelial cells (purple), NH-A: normal human astrocytes (orange), NHDF:

normal human dermal fibroblasts (red), NHEK: normal human epidermal keratinocytes (fuchsia),

Osteobl: normal human osteoblasts (royal blue).
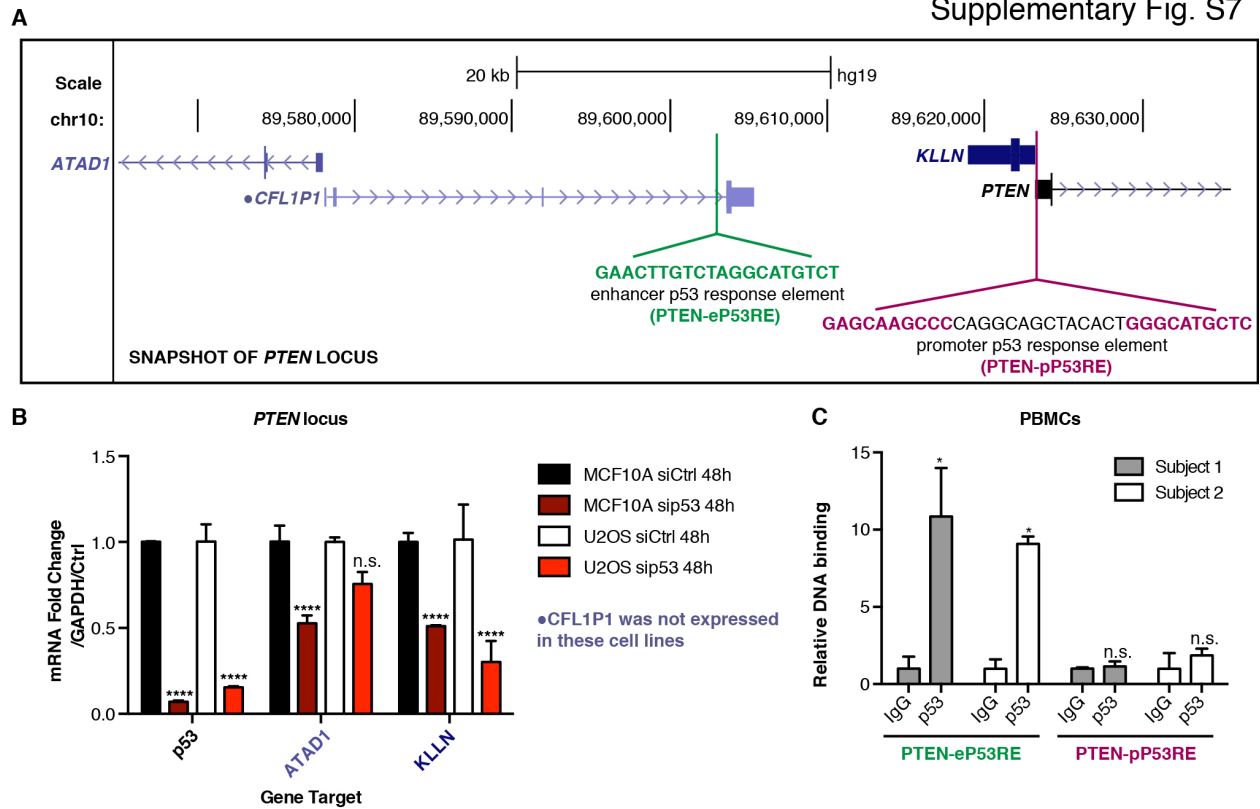
Supplementary Fig. S7: The binding and regulation of the *PTEN* locus by basal p53. (A) Map of the *PTEN* genomic locus adapted from the UCSC genome browser (57) including genes upstream of *PTEN* that are near the basal p53 binding site. **(B)** MCF10A and U2OS cells were transfected with control or p53-targeting siRNAs (pool of 4 siRNAs), qRT-PCR was used to measure transcript levels of ATAD1, CFL1P1, and KLLN. Error bars: mean ± s.d. of representative experiment (performed twice for each cell line), triplicate measurements. Significance: two-way ANOVA, Sidak's correction. **(C)** ChIP-qPCR in PBMCs from two healthy donors (Subjects 1 and 2) for basal p53 on PTEN-eP53RE and PTEN-pP53RE. Relative DNA Binding is % input (normalized to IgG). Error bars: mean ± s.d., triplicate measurements. Significance (over IgG): two-way ANOVA, Dunnett's correction. (****p≤.0001, *p≤.05, n.s. p>.05)

Supplementary Fig. S8

A

Consensus Motif

RRRCWWGYYY ———— 0-14 bp spacer ———— RRRCWWGYYY

R=purine, W=adenine or thymine, Y=pyrimidine

B Conservation of PTEN-eP53RE

```
Human      GAACTTGTCTAGGCATGTCT
Chimp      GAACTTGTCTAGGCATGTCT
Gorilla    GAACTTGTCTAGGCATGTCT
Marmoset   GAACTTGTCTAGGCATGTCT
Tree Shrew GGACATGTCCAGGCATGTCT
Guinea Pig AAACCTGTCTAGGCATGTCT
Rhinoceros GGGCCTGTATGGGCATGTCT
Dog        GGACCTGTGTGGGCATGTCT
Hedgehog   GGACATGTCGGGACATGTCT
Elephant   GGGCCTGTTAGGGCATGTCT
Manatee    GGGCCTGTTAGGGCATGTCT
Armadillo  GGGCCAGCCTGGGCATGTCT
           ****  ***  **********
```

C U2OS PTEN-eP53RE

D MCF10A PTEN-eP53RE
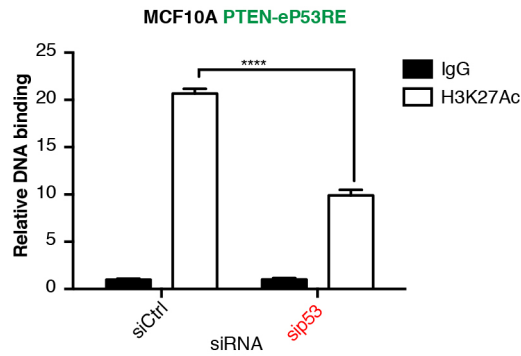
Supplementary Fig. S8: PTEN-eP53RE is a highly conserved p53 response element in a p53-dependent enhancer. (A) p53 consensus sites are typically two 10 base pair palindromic repeats separated by a 0-14bp spacer (59). **(B)** PTEN-eP53RE is highly conserved in mammals (Multiz alignment shown). **(C-D)** ChIP-qPCR for H3K27Ac on PTEN-eP53RE in cells transfected with control or p53-targeting siRNA (pool of 4 siRNAs) in U2OS **(C)** and MCF10A **(D)** cells. Relative DNA binding is % input (normalized to IgG). Error bars: mean ± s.d. of representative experiment (performed twice), triplicate measurements. Significance: two-way ANOVA, Sidak's correction. (****p≤.0001, n.s. p>.05)

A Deletion of PTEN-eP53RE in cases from TCGA using Integrative Genomics Viewer

Supplementary Fig. S9

Tumor Type (TCGA)	TCGA Case	PTEN CN	eP53RE CN	TP53 MUT	PTEN mRNA	Size of del.
LGG	TCGA-HT-7690-01	0	-.7797	Y236C	-1.4078	~5kb
STAD	TCGA-BR-8058-01	0	-.4515	WT	-0.6392	~800kb

B

C
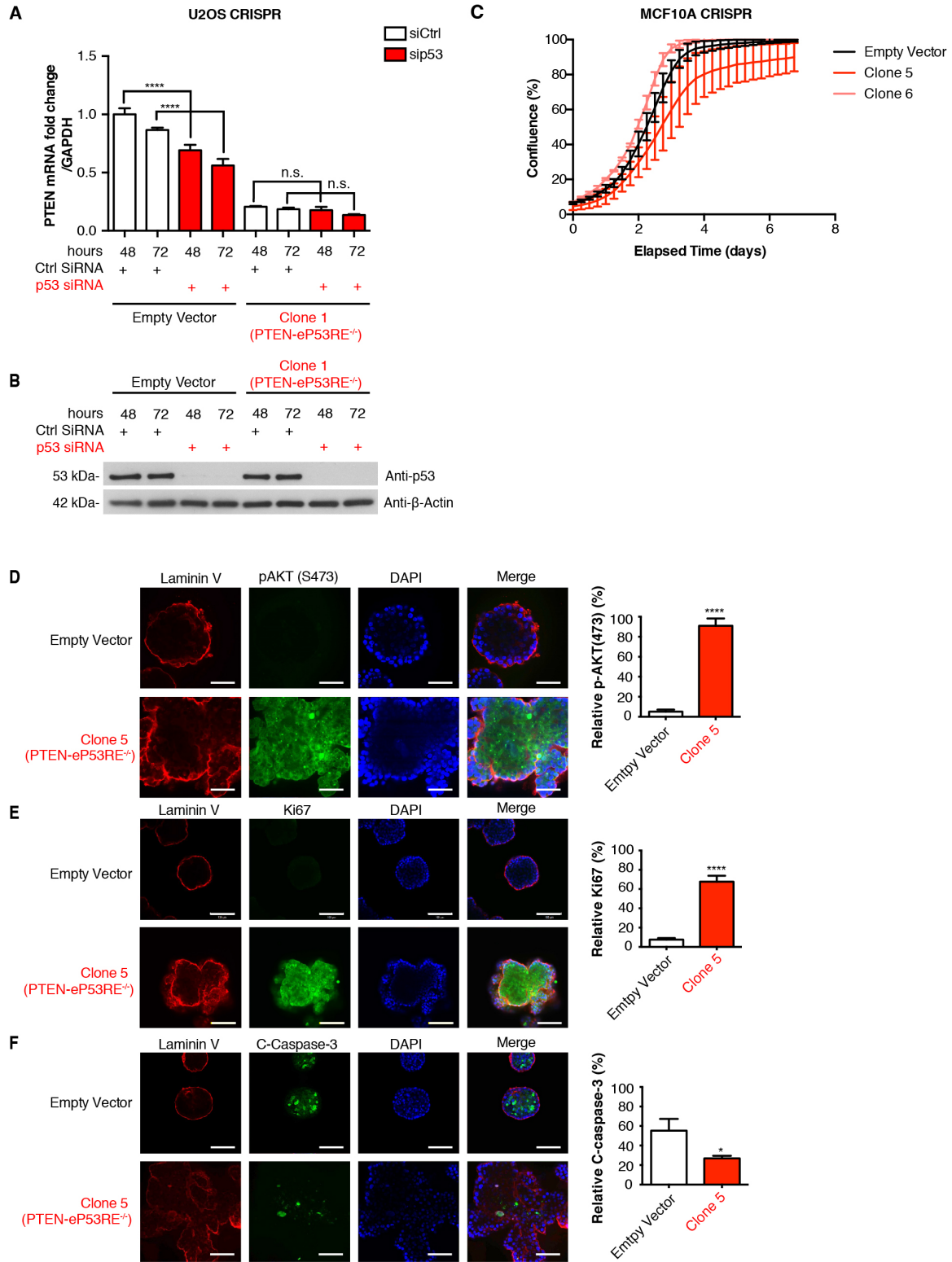
Supplementary Fig. S9: Deletion of endogenous PTEN-eP53RE by CRISPR/Cas9. (A) There were 2 cases from TCGA harboring deletions (deep deletions, likely homozygous determined by GISTIC2.0 (60)) in PTEN-eP53RE. Table contains (by column, left to right) the type of cancer, TCGA case number, the IGV-scaled copy number data for *PTEN* and PTEN-eP53RE (log_2(tumor signal / normal signal), the *TP53* status, the PTEN mRNA z-score by RNA-seq, and the approximate size (in kb) of the deletion. **(B)** The dual expression vector LentiCRISPRv2 containing CRISPR/Cas9 and sgRNA targeting PTEN-eP53RE was used to create modifications in the PTEN-eP53RE locus. **(C)** Sequences of clones generated using CRISPR/Cas9 in U2OS (top) and MCF10A (bottom) cells. Homozygous deletions in PTEN-eP53RE (PTEN-eP53RE$^{-/-}$) are shown in red.

Supplementary Fig. S10

A U2OS CRISPR

B

C MCF10A CRISPR

D Laminin V | pAKT (S473) | DAPI | Merge

E Laminin V | Ki67 | DAPI | Merge

F Laminin V | C-Caspase-3 | DAPI | Merge

Supplementary Fig. S10: Depletion of p53 causes a PTEN-eP53RE-dependent decrease in PTEN expression, deletion of PTEN-eP53RE alters some tumor cell phenotypes. (A) U2OS Empty Vector or Clone 1 (PTEN-eP53RE$^{-/-}$) cells were transfected with control or p53-targeting siRNA (pool of 4 siRNAs) and qRT-PCR was used to measure PTEN transcript levels 48h and 72h after transfection. Error bars: mean ± s.d., triplicate measurements. Significance: one-way ANOVA, Sidak's correction. **(B)** Western blot for p53 showing that p53 was effectively knocked down at 48h and 72h after transfection in both cell lines. β-actin was a loading control. **(C)** Proliferation assay of MCF10A clones in low serum showing % confluence over time (days). Triplicate readings taken every 6 hours. Error bars: mean ± s.d. **(D-F)** MCF10A clones grown in 3D culture for 20 days. Representative immunofluorescence staining for Laminin V (red, all rows, **(D)** pAKT(Ser473), **(E)** Ki67, and **(F)** cleaved Caspase-3 (green), DAPI (blue, all rows), merge (right, all rows). Scale bars: 100µm. Quantifications on right. Empty Vector data is identical to Fig. 5G-I. Error bars: mean ± s.d. of representative experiment, triplicate measurements. Significance: two-tailed t-test. (****p≤.0001, *p≤.05, n.s. P>.05)

Supplementary Tables S1-S3:

Gene Name	GEMM of TS?	Inherited cancer syndrome?	Somatic mut in cancer?	Somatic mut Lawrence *et al*(61)
CDKN1A(p21)	Y(62)	N	Y(63,64)	Y
DLEU1	Y(65,66)	N	Y(67)	N
SMARCA2	Y(68)	N	Y(69-71)	N
PTEN	Y(72,73)	Y(74)	Y(75,76)	Y
FAT1	N	N	Y(77,78)	Y
KDM6A(UTX)	N	N	Y(79-81)	Y
miR-34	Y(82,83)	N	Y(84,85)	N
TNFRSF10B	Y(86)	N	Y(87-89)	N
STK11(LKB1)	Y(90,91)	Y(92)	Y(93-95)	Y
PHLDA3	Y(96)	N	Y(96)	N
WT1	Y(97)	Y(98)	Y(99,100)	Y
FOXO1	Y(101)	N	Y(102-104)	N
BMPR1A	Y(105,106)	Y(107,108)	Y(109)	N

Supplementary Table S1: Information on tumor suppressor genes identified as basal p53 targets. The list of genes contained within this table are well-validated tumor suppressors based on experimental evidence (columns from left to right) from genetically engineered mouse models (GEMM), inherited cancer predisposition syndromes driven by germline mutations, somatic mutations in human cancer, and somatic mutations in the pan-cancer Lawrence *et al(61)* study. Each cell is labeled as yes or no (denoted 'Y' or 'N', respectively) and the 'Y' cells contain supporting references.

Gene Name	Peak Location (MCF10A)	JASPAR MA0106.3 sequence (+)	Score (+)	Rel. Score (+)
PLAC8	Chr4: 84092183-84092485 RE1:	CACATGCCTGGACATGCC	20.762	0.934
	RE2:	GGCATGCCTGGACATGTC	23.696	0.961
TGFA	Chr2: 70824017-70824382	AACATGCCCAGGCATGTC	26.586	0.988
CDKN1A(p21) 5'	Chr6: 36644096-36644510	AACATGTCCCAACATGTT	21.840	0.944
DLEU1	Chr13: 51103523-51103774	GGCTTGTCCGGGCATGTC	20.946	0.936
SMARCA2	Chr9: 1707411-1707559	AACATGCCTGGGCTTGCC	20.450	0.932
PTEN	Chr10: 89602953-89603111	AACTTGTCTAGGCATGTC	20.235	0.930
PLK2	Chr5: 57758019-57758216	GGCAAGTCCAGGCATGTT	20.085	0.928
BRD1	Chr22: 501153990-50154296	GACATGCCTAAACATGCC	19.717	0.925
JAG1	Chr20: 10713952-10714118	GGCTAGCCCGGGCATGTT	18.251	0.912
KDM6A(UTX)	ChrX: 44835018-44835187	GGCTTGCCTGGGCATGCC	17.648	0.906
miR-34	Chr1: 9242010-9242446	AACAAGCCCAGGCAAGCC	17.471	0.904
TNFRSF10B	Chr8: 22926070-22926238	GTCTTGCCCGGACATGCC	17.301	0.903
VAV2 Peak 2	Chr9: 136753460-136753626	GGCAGGCCCAGACATGTC	17.192	0.902
STK11(LKB1)	Chr19: 1210487-1210722	GGCATGTTCGGTCATGCC	14.493	0.877
CCNG1	Chr5: 162864877-162865038	CACAAGCCCAGGCTAGTC	13.611	0.869
TGFB2	Chr1: 218774483-218774664	GACAAGTCTGAACTTGCC	13.439	0.868
PHLDA3	Chr1: 201438170-201438422	GATGTGCCCTTACATGTT	13.091	0.865
NOTCH1	Chr9: 139444765-139445192	GAGTTGCCCGGGCAAGTC	11.830	0.853
WT1	Chr11: 32325276-32325457	GGCATGTTAGCACATGCC	11.649	0.851
PLK3	Chr1: 45265510-45265694	AACATGCCCGGGCAAAAG	11.134	0.847
VAV2 Peak 1	Chr9: 136746439-136746521	AATGTGTCTGGACTTGCC	10.762	0.843
FOXO1	Chr13: 40907488-40907636	GGCATGTCGGGGCATCAC	9.905	0.835
CDKN1A(p21) 3'	Chr6: 36644988-36645255	AAGAAGACTGGGCATGTC	8.728	0.825
MDM2	Chr12: 69202725-69202891	GTCAAGTTCAGACACGTT	8.524	0.823
FAT1	Chr4: 187841713-187841958	GACATGCCCGGGCAAAGG	8.332	0.821
BMPR1A	Chr10: 88566579-88566727	ATGTTGGCCAGGCTTGAT	-3.982	0.709

Supplementary Table S2: Predicted p53 response elements within basal p53 binding sites using JASPAR. Using the HOMER-annotated list of basal p53 peaks from MCF10A and U2OS cells, we used JASPAR software to scan the region of DNA containing the p53 peak for potential p53 response element sequences. This table contains (by column, left to right) the gene name, the location of the called peak, the predicted p53 response element sequence (the exact output of the program using the matrix model MA0106.3), the score of that binding site based on position-weight matrix, and the relative score. Note: The JASPAR program output for matrix model MA0106.3 is a sequence that lacks the outer two base pairs of the known consensus sequence (110) (RRRCWWGYYY-RRRCWWGYYY, where R=purine, Y=pyrimidine, W=adenine or thymine).

51

Gene Name	Peak Location		H3K27Ac	H3K4me1	H3K4me3	~bp to TSS	Description
CDKN1A(p21) 5'	Chr6: 36644096-36644510	Intergenic	+	+	+	1.9 kb	Enhancer
CDKN1A(p21) 3'	Chr6: 36644988-36645355	near TSS	+	+	+	1.1 kb	Promoter
DLEU1	Chr13: 51103523-51103774	Intergenic	+	+	+	450 kb	Enhancer
SMARCA2	Chr9: 1707411-1707559	Intergenic	+	+	-	300 kb	Enhancer
PTEN	Chr10: 89602953-89603111	Intergenic	+	+	-	20 kb	Enhancer
FAT1	Chr4: 187841713-187841958	Intergenic	+	+	-	200 kb	Enhancer
KDM6A(UTX)	ChrX: 44835018-44835187	Intronic	+	+	-	100 kb	Enhancer
miR-34	Chr1: 9242010-9242446	near TSS	+	-	+	0 bp	Promoter
TNFRSF10B	Chr8: 22926070-22926238	near TSS	+	-	+	462 bp	Promoter
STK11(LKB1)	Chr19: 1210487-1210722	Intronic	+	+	-	5kb	Enhancer
PHLDA3	Chr1: 201438170-201438422	near TSS	+	-	+	0 bp	Promoter
WT1	Chr11: 32325276-32325457	Intergenic	-	+	-	130 kb	Enhancer
FOXO1	Chr13: 40907488-40907636	Intergenic	+	+	+	330 kb	Enhancer
BMPR1A	Chr10: 88566579-88566727	Intronic	-	-	-	50 kb	Unknown

Supplementary Table S3: Chromatin properties of basal p53 binding sites near tumor suppressor genes. p53-bound DNA near tumor suppressor genes was analyzed for the presence of H3K27Ac, H3K4me1, and H3K4me3 marks, and for the distance from the transcriptional start site (bp from TSS) in hMEC cells. We have indicated (columns left to right) the gene name, the genomic location of the peak, if the peak overlaps with H3K27Ac, H3K4me1, and/or H3K4me3 (Pos or Neg, +/-), distance from the TSS, and the classification of the element. Element was classified as 'promoter' if distance from TSS is <1.5kb and is '+' for H3K4me3. Element was classified as 'enhancer' if distance from TSS is >1.5kb and is '+' for H3K4me1 (active enhancers are also '+' for H3K27Ac). Others are classified as 'unknown'. Data is available from Broad/ENCODE (54,57,58).

Supplementary Spreadsheets S1-S5 (Large Excel spreadsheets uploaded as separate files):

Supplementary Spreadsheet S1: Basal p53 ChIP-seq peaks in MCF10A cells (after raw data analysis described in Materials in Methods section) ordered by significance of the peak call. Spreadsheet includes (columns left to right) peak locus (Chromosome, start, end), MACS2 significance, closest relevant gene (genes discussed in paper in red type), and original HOMER gene call (if relevant gene differs from called gene).

Supplementary Spreadsheet S2: Basal p53 ChIP-seq peaks in U2OS cells (after raw data analysis described in Materials in Methods section) ordered by significance of the peak call. Spreadsheet includes (columns left to right) peak locus (Chromosome, start, end), MACS2 significance, closest relevant gene (genes discussed in paper in red type), and original HOMER gene call (if relevant gene differs from called gene).

Supplementary Spreadsheet S3: List of tumor suppressor genes and oncogenes derived from the gene classifications of the Cancer Gene Census in COSMIC (used in GSEA). Spreadsheet shows gene name and classification (tumor suppressor gene or oncogene).

Supplementary Spreadsheet S4: List of genes deleted at a frequency of 0.5% or greater in all cancer types in TCGA (used in GSEA). Acronyms for cancer types are expanded in the Materials and Methods.

Supplementary Spreadsheet S5: List of genes amplified at a frequency of 0.5% or greater in all cancer types in TCGA (used in GSEA). Acronyms for cancer types are expanded in the Materials and Methods.

Supplementary Materials and Methods

Cell Culture:

MCF10A cells were cultured in 50/50 DMEM/Ham's F-12 media with 5% horse serum (Gibco 16050-122), 1X Penicillin/Streptomycin (Corning 30-002-Cl), 20 ng/ml of EGF (Peprotech AF-100-15), 10 µg/ml insulin (Sigma I9278), 0.5 mg/ml hydrocortisone (Sigma H0888), and 100 ng/ml cholera toxin (Sigma c8052). U2OS cells were cultured in 1X DMEM with 10% fetal bovine serum (Atlanta Biologicals S11150) and 1X Penicillin/Streptomycin. HCC38 cells were cultured in 1X RPMI with 10% fetal bovine serum and 1X Penicillin/Streptomycin. Cells were split using 0.05% or 0.25% trypsin (Corning 25-051-Cl or 25-053-Cl, respectively) before they reached full confluence and media was changed every 3-4 days. Corning Cellgro Media product information is as follows, DMEM: 10-013-CV, RPMI: 10-040-CV, 50/50 DMEM/ Ham's F-12: 10-090-CV. Human mammary epithelial cells were derived using the Schlegel method as described(111). Instead of using conditioned media + cells, only conditioned media was used.

Nutlin**:** Nutlin-3 (Sigma Aldrich, N6287-5MG) was dissolved in DMSO and was used at a concentration of 10 µM in media for indicated time. Control is treatment with equal volume of DMSO.

Transient Knockdown of p53:

SMARTpool: ON-TARGET plus Human TP53 siRNA (L-003329-00-0020) (pool of 4 siRNAs) and ON-TARGET plus Human TP53 siRNA (J-003329-15 and J-003329-17 for individual siRNAs #1 and #2, respectively) were used to transiently knock down p53. The lipofectamine, Opti-MEM, and siRNA were mixed together and incubated at room temperature for 30 minutes. The mixture was added dropwise to cells already containing an equal volume of the fully supplemented media without antibiotics. This media was left on the cells for 5-16 hours and was subsequently changed to fully supplemented media with antibiotics.

Human Tissue Samples:

De-identified breast cancer tissue samples were distributed by the Tumor Bank in the Herbert Irving Comprehensive Cancer Center Molecular Pathology Shared Resource. De-identified peripheral blood mononuclear cells (PBMCs) from healthy donors were distributed by the Immune Monitoring Core at Icahn School of Medicine at Mount Sinai.

Plasmids for Luciferase Reporter Assay:

p53 Expression Plasmid:

The **pC53-pSN3** plasmid (previously published (112), gift from Dr. Bert Vogelstein) was used to overexpress p53 where WT p53 cDNA was cloned into the unique Bam H1 site in the expression vector **pCMV-Neo** (empty vector) to produce **pC53-SN3**.

Luciferase Plasmid:

The **pGL3** basic reporter vector is commercially available (ProMega). The construction of **pGL3-EibTATA** (a pGL3 based luciferase reporter under the control of the minimal adenovirus E1b promoter) and **pGL3-E1bTATA-p21 5'** have been previously described (113).   The plasmids, **pGL3-TATA-Hu PTEN-eP53RE** (GAACTTGTCTAGGCATGTCT), **pGL3-TATA-Hu PTEN-pP53RE** (GAGCAAGCCCCAGGCAGCTACACTGGGCATGCTC) were constructed by synthesizing and cloning oligonucleotides with *Xho1* and *Nhe1* ends into the polylinker of **pGL3-E1bTATA**.

CRISPR of Hu PTEN-eP53RE:

Guide Sequences:

CACCGTAGGCATGTCTAGTGAGCAA

AAACTTGCTCACTAGACATGCCTAC (complimentary)

Lentivirus was produced in HEK-293T cells as previously described (114) by transfecting 0.3 μg of **VSV-G,** 3 μg of **pCMV-DR8.9**, and 3.6 μg of **p53-PTEN-LentiCRISPRv2** or empty **LentiCRISPRv2** into a 10cm plate of cells and collecting viral particles from media 24 and 48 hours post-transfection. The viral media was filtered through a .45 micron syringe filter (Fisher 194-2545) and stored at -80°C. Viral media was used to infect mammalian cells in the presence of 12μg/mL polybrene and 2 μg/mL of puromycin (Sigma P8833) was used to select for infected cells. Limiting dilution was used to isolate single colonies, DNA from which was amplified and sequenced by Genewiz using the primers listed below.

PCR Primers:

For: GGAATGCTTCAGTCTGCTCC

Rev: TCTGGCATGTTTGCATTTTC

Sequencing Primers:

For: ATGGCCACAACCCTTATTCC

Rev: TTTGCTGCTACACTGCTTCC

If the CRISPR deletion was too large to use the sequencing primers, then the PCR

product was purified and the PCR primers were used for sequencing. Selected clones

were used for further experiments.

Conservation Analysis:

Multiz alignment was run from the UCSC genome browser for selected organisms as

previously described (115).

RT-qPCR:

RNA was prepared using the QiaShredder (79654) followed by the Qiagen RNeasy Kit

(74104). cDNA was synthesized using the SuperScript Reverse Transcriptase II kit

(Thermo 18064-014). The Applied Biosystems 7500 Fast Quantitative Realtime PCR

System was used according to manufacturers' protocol using Fast SYBR Green Master

Mix (Thermo 4385612). All qRT-PCR values were normalized to GAPDH.

The temperature program was as follows:

Initial Denaturation: 95°C 20sec

40 cycles: 95°C 3sec, 60°C 30sec

qRT-PCR Primers:

p53-For: CTTTGAGGTGCGTGTTTGTG

p53-Rev: GGGCAGTGCTCGCTTAGT

CDKN1A(p21)-For: ACTCTCAGGGTCGAAAACGG

CDKN1A(p21)-Rev: CCTCGCGCTTCCAGGACTG

BBC3(PUMA)-For: CGGCGGAGACAAGAGGAG

BBC3(PUMA)-Rev: CAGGGCTGGGAGTCCAGTAT

MDM2-For: CTGTGTTCAGTGGCGATTGG

MDM2-Rev: AGGGTCTCTTGTTCCGAAGC

miR-34a-For: AGTCCTGCAGCCAAGCTC

miR-34a-Rev: TGTCCTGCCTCTCCCCAG

BMPR1A-For: ACTGCCCCCTGTTGTCATAG

BMPR1A-Rev: AGCAATTATGCAGACAGCCA

PHLDA3-For: CAGCTGTGGAAGCGGAAG

PHLDA3-Rev: GCGAAGCTGAGCTCCTTG

CCNG1-For: CTCCTTCAAGAGAACTTGCCA

CCNG1-Rev: TGACATGCCTTCAGTTGAGC

GADD45a-For: ACTTATTTGTTTTTGCCGGG

GADD45a-Rev: ATTCAGATGCCATCACCGTT

NOTCH1-For: GGCAATCCGAGGACTATGAG

NOTCH1-Rev: CAGAACGCACTCGTTGATGT

TGFA-For: TAATGACTGCCCAGATTCCC

TGFA-Rev: TACCCAGAATGGCAGACACA

PLK3-For: GCGCGAGAAGATCCTAAATG

PLK3-Rev: TTGTCAGCGTCCTCAAAGTG

PTEN-For: CCAGTCGCTGCAACCATC

PTEN-Rev: CTTCTTCTGCAGGATGGAAATG

STK11(LKB1)-For: TGCTGAAAGGGATGCTTGAGTA

STK11(LKB1)-Rev: GGATGGGCACTGGTGCTT

KDM6A(UTX)-For: CATGGTGTTCAATAGGTGTGCT

KDM6A(UTX)-Rev: CCATGGTCCAATTGTACAGC

FAT1-For: GGGTGAGCTCCACGAGAG

FAT1-Rev: CAAATGTCTCCCCATTGCTT

FOXO1-For: AAGGGTGACAGCAACAGCTC

FOXO1-Rev: TTCCTTCATTCTGCACACGA

JAG1-For: AGTGTGATACCAGATGGGGC

JAG1-Rev: ACACCAGACCTTTGAGCAGG

TGFB2-For: CATCTACAACAGCACCAGGG

TGFB2-Rev: GGCGTAGTACTCTTCGTCGC

VAV2-For: CGCTTTGCAATAAGCATCAA

VAV2-Rev: TGGCCTCTGTGATGTGGAT

BRD1-For: ACTGATCATCGACCCCAAGA

BRD1-Rev: ATGTGCTCCCCAATCTTCAG

PLAC8-For: CGTCGCAATGAGGACTCTCT

PLAC8-Rev: GAGGACAGCAAAGAGTTGCC

PLK2-For: AATAACAAAGTCTACGCCGCA

PLK2-Rev: TCTTTGTCAATCTTTTCCCTTTG

TNFRSF10B-For: CAGAGCCAACAGGTGTCAAC

TNFRSF10B-Rev: GCCTCCTCCTCTGAGACCTT

KLLN-For: GGACCACAGTGGAAAAGGAA

KLLN-Rev: TCTGGAAATCAACTGGAGGC

CFL1P1-For: TCCTTCAGACAGAGTCGGGT

CFL1P1-Rev: GAGGCTGCAGTGGTCATTGT

GAPDH-For: TCACCAGGGCTGCTTTTAAC

GAPDH-Rev: AATGAAGGGGTCATTGATGG

Immunoblotting:

Cells were lysed in 2x sample buffer (125 mM Tris-HCl at pH 6.8, 10% βME, 2% SDS, 20% glycerol, 0.05% Bromophenol Blue, 8 M urea). Protein lysates were loaded into 4-20% TRIS-glycine gels and resolved by electrophoresis. Samples were then blotted on PVDF membrane (Millipore IPVH00010) using the wet transfer technique (Invitrogen). Membranes were blocked in 5% milk-TBST for 1 hour, washed in TBST for 10 minutes, and incubated in primary antibody in 5% milk-TBST or 5% BSA-TBST at 4°C for 16 hours. Membranes were rinsed (3 x 6 min) in TBST, incubated in horseradish peroxidase-conjugated secondary antibodies in 5% milk-TBST for 1 hour, and rinsed again in TBST (3 x 6 min). Membranes were visualized using the chemiluminescence system (Thermo 34080, 37075) on autoradiography film (Denville E3018). Blots were quantified using ImageJ.

Primary Antibodies: Vinculin (Sigma V9131), β-actin (Sigma A5316), PTEN (138G6, CST 9559), pAKT (Thr308 CST 9275, Ser473 CST 9721), total AKT (CST 9272), p53 (DO-1, SC-126), p21 (C-19, SC-397), LKB1 (CST 3050), KDM6A/UTX (CST 33510).

Secondary Antibodies: Mouse (Thermo 31432), Rabbit (Thermo 31460).

Chromatin Immunoprecipitation (ChIP-qPCR and ChIP-sequencing):

ChIP-qPCR Primers:

PTEN-eP53RE-For: CACATAAAGGCTGCATTCACA

PTEN-eP53RE-Rev: TTCCTAGCAGACTCCTCCCA

PTEN-eP53RE-Rev (Alt): CTCCCTAAGGTTTCCAGTATTCTG (for U2OS CRISPR

Clone 3)

PTEN-pP53RE-For: CAAAAGCCGCAGCAAGTG

PTEN-pP53RE Rev: TGAGCATGCCCAGTGTAGC

5'CDKN1A-eP53RE-For: CTGGACTGGGCACTCTTGTC

5'CDKN1A-eP53RE-Rev: CTCCTACCATCCCCTTCCTC

STK11(LKB1)-For: GCTCTCACCGGCAAAAAGTA

STK11(LKB1)-Rev: GCCCAGCCCTCTTTTTAACT

Analysis of ChIP-seq data:

ChIP-seq reads were aligned to the genome using Bowtie (Version 2.2.3). Hg19 was

used as the reference genome. For p53 alignments, all default parameters were used.

MACS2 Version 2.1.0 was used to call significant peaks, and the narrow peak option was

used with the following parameters: p53 peaks: -B --SPMR --nomodel --extsize 150 --

keep-dup 2. All other parameters were run in the default setting. Initial output of MACS2

is a pileup value. MACS2 determines peak significance using a binomial test to

determine p-value at each genomic location followed by the Benjamini-Hochberg

procedure to control for FDR (q-value). MACS2 was also used to calculate fold

enrichment scores (IP sample over input across genome) using the bdgcmp FE function.

Plots to visualize the data were generated by the UCSC genome browser and adapted in

Illustrator. Nearest genes to peaks were called using HOMER software(116). MCF10A

cells and DMSO-treated U2OS cells were used as starting material for the two basal p53

ChIP-seq data sets. The U2OS (DMSO- treated) p53 ChIP-seq data set was previously

published(52) and can be accessed from the Gene Expression Omnibus (GEO) using the

accession number GSE46641. We chose to analyze the U2OS DMSO-treated dataset over

the 'no treatment' (NT) dataset from the same study because the NT dataset did not

contain peaks for *CDKN1A (p21)* or *mIR-34a*, two genes that are known to be regulated

by basal p53; suggesting that the U2OS NT data set does not meet the quality standards

required for analysis.

Sample	Sequenced Reads	Aligned Reads
MCF10A input	57,840,295	55,854,243
MCF10A p53	27,482,537	25,976,864
U2OS DMSO input	34,268,308	32,009,064
U2OS DMSO p53	39,717,260	36,629,383

Broad/ENCODE ChIP-seq data:

Data for various histone modifications (H3K27Ac, H3K4me1, H3K4me3) in various cell

lines were adapted from the UCSC Genome Browser under the 'Encode Histone

Modifications' track set (54,57,58). GEO accession numbers can be accessed for each

cell line and histone mark via the UCSC genome browser under 'configure track set'.

Chromatin State Segmentation (ChromHMM) and Hi-C:

Chromatin state tracks were produced by the ENCODE project(54), see original

publication for description of classification strategy(57,117). Hi-C data was also

previously published(53), and can be accessed through the GEO accession GSE63525.

Both ChromHMM and Hi-C data were adapted from the WashU genome browser(55,56).

The color key for ChromHMM data is as follows:

1		Active TSS
2		Flanking Active TSS
3		Transcr at gene 5' and 3'
4		Strong transcription
5		Weak transcription
6		Genic enhancers
7		Enhancers
8		ZNF genes & repeats
9		Heterochromatin
10		Bivalent/Poised TSS
11		Flanking Bivalent TSS/Enh
12		Bivalent Enhancer
13		Repressed PolyComb
14		Weak Repressed PolyComb
15		Quiescent/Low

p53 response element prediction:

We used a program called JASPAR that uses position-weight matrix (PWM) to identify

and assign a score to potential p53 response elements, as has been previously described

(118). The matrix model MA0106.3 was used to predict p53 binding sites.

Proliferation assay:

U2OS cells (Empty Vector and Clone 1) were plated at 2000 cells/well in 96-well tissue

culture plates (Corning 3595) media containing 1% FBS (low serum). Cells were allowed

to grow for the indicated number of days. The Essen BioScience IncuCyte® ZOOM Live-Cell Analysis System took phase-contrast images in triplicate wells every 6 hours. The IncuCyte® software package was used to estimate confluence at each time point.

Soft agar assay:

U2OS empty vector cells and subclones were trypsinized and resuspended in 2X DMEM media. The bottom layer consisted of 1 ml/well of 0.7 % agar noble (Difco 214220) for 24-well plate. The cell suspensions were cultured in a 0.3 % agar noble (1ml/well) and layered on top. The cells were maintained in an incubator for 21 days. The colonies were stained with 0.005% Crystal Violet, photos were taken, and colonies were counted with ImageJ. The experiments were independently performed at least twice, each in triplicate.

Abbreviations for Cancer Types in The Cancer Genome Atlas:

SKCM: skin cutaneous melanoma, LGG: brain lower-grade glioma, BRCA: breast invasive carcinoma, LAML: acute myeloid leukemia, PRAD: prostate adenocarcinoma, GBM: glioblastoma mutliforme, KIRP: kidney renal cell papillary carcinoma, THCA: thyroid carcinoma, KIRC: kidney renal clear cell carcinoma, STAD: stomach adenocarcinoma, CESC: cervical squamous cell carcinoma and endocervical adenocarcinoma, BLCA: bladder urothelial carcinoma, LIHC: liver hepatocellular carcinoma, OV: ovarian serous cystadenocarcinoma, LUSC: lung squamous cell carcinoma, LUAD: lung adenocarcinoma, HNSC: head and neck squamous cell carcinoma, PAAD: pancreatic adenocarcinoma.

Gene Set Enrichment Analysis of MCF10A basal p53 ChIP-seq dataset:

Tumor suppressor genes (TSGs) and oncogenes were classified in the Cancer Gene

Census from COSMIC (119) (as of January 4th, 2017). Frequencies of somatic copy-loss

and copy-gain by gene were retrieved from the cBio portal, averaged across 18 cancer

types, and thresholded at 0.5% mean frequency to yield gene sets of the most recurrently

deleted and amplified genes in TCGA. Enrichment of the list of MCF10A ChIP-seq

peaks (ranked by significance) for these gene sets of TSGs and oncogenes, or recurrent

deletions and amplifications was quantified using the Gene Set Enrichment Analysis

package (120).

Analysis of odds of basal p53 target downregulation in cases with *TP53* mutation:

We restricted our analysis to the TCGA cases for which exome sequencing, SNP array,

and RNA sequencing data were all available, and queried the mutational status of *TP53*

along with the expression levels of its target tumor suppressors. Contingency tables were

constructed between *TP53* mutation status and target gene expression z-scores,

thresholded at -1 standard deviation. Associations were quantified via Fisher's exact test.

Cancer types that were included in this analysis had sufficient data and cases available.

Copy Number Variation (PTEN-eP53RE):

cBioPortal was used to identify TCGA cases with decreased copy number of PTEN-

eP53RE, where "deep deletions" are most likely homozygous deletions and "shallow

deletions" are most likely heterozygous deletions. Both of the identified cases harbored

"deep deletions" in PTEN-eP53RE. cBioPortal uses GISTIC2.0 to identify copy number

changes (60). Integrative Genomics Viewer (IGV) was used to estimate the specific location and size of the deletion, and to provide the IGV-scaled CNV numbers, which reflect $\log_2$(tumor signal / normal signal) (121,122).

Statistical Analysis:

No statistical methods were used to determine sample size, and experiments were not randomized or blinded. Aside from traditional Mann-Whitney (non-parametric), Spearman correlation test (non-parametric), student t-tests (parametric) to compare two data sets, and Chi-squared test (non-parametric), parametric statistical methods were used in order to make appropriate multiple comparisons of repeated measures of data (following 1-way or 2-way ANOVA as indicated in figure legends). Graphpad Prism was used to make these simple predetermined statistical comparisons.

Dunnett's Multiple Comparisons Correction: Used for comparing all samples to a control sample, but not for comparing the non-control samples to one another.

Sidak's Multiple Comparisons Correction: Used when specific multiple comparisons are pre-selected.

Fischer's Exact Test: Used to analyze the Odds Ratio data from TCGA cases (displayed in a contingency table).

Supplementary References:

51.   Saal LH, Johansson P, Holm K, Gruvberger-Saal SK, She QB, Maurer M*, et al.* Poor prognosis in carcinoma is associated with a gene expression signature of aberrant PTEN tumor suppressor pathway activity. *Proceedings of the National Academy of Sciences* **2007**;104:7564-9.

52. Menendez D, Nguyen TA, Freudenberg JM, Mathew VJ, Anderson CW, Jothi R*, et al.* Diverse stresses dramatically alter genome-wide p53 binding and transactivation landscape in human cancer cells. *Nucleic Acids Res* **2013**;41:7286-301.

53. Rao SS, Huntley MH, Durand NC, Stamenova EK, Bochkov ID, Robinson JT*, et al.* A 3D map of the human genome at kilobase resolution reveals principles of chromatin looping. *Cell* **2014**;159:1665-80.

54. ENCODE. An integrated encyclopedia of DNA elements in the human genome. *Nature* **2012**;489:57-74.

55. Zhou X, Maricque B, Xie M, Li D, Sundaram V, Martin EA*, et al.* The Human Epigenome Browser at Washington University. *Nat Methods* **2011**;8:989-90.

56. Zhou X, Lowdon RF, Li D, Lawson HA, Madden PA, Costello JF*, et al.* Exploring long-range genome interactions using the WashU Epigenome Browser. *Nat Methods* **2013**;10:375-6.

57. Kent WJ, Sugnet CW, Furey TS, Roskin KM, Pringle TH, Zahler AM*, et al.* The Human Genome Browser at UCSC. *Genome Res* **2002**;12:996-1006.

58. Ram O, Goren A, Amit I, Shoresh N, Yosef N, Ernst J*, et al.* Combinatorial patterning of chromatin regulators uncovered by genome-wide location analysis in human cells. *Cell* **2011**;147:1628-39.

59. Kern SE, Kinzler KW, Bruskin A, Jarosz D, Friedman P, Prives C*, et al.* Identification of p53 as a Sequence-Specific DNA-Binding Protein. *Science* **1991**;252:1708-11.

60. Mermel CH, Schumacher SE, Hill B, Meyerson ML, Beroukhim R, Getz G. GISTIC2.0 facilitates sensitive and confident localization of the targets of focal somatic copy-number alteration in human cancers. *Genome Biol* **2011**;12:R41.

61. Lawrence MS, Stojanov P, Mermel CH, Robinson JT, Garraway LA, Golub TR*, et al.* Discovery and saturation analysis of cancer genes across 21 tumour types. *Nature* **2014**;505:495-501.

62. Martın-Caballero J, Flores JM, Garcia-Palencia P, Serrano M. Tumor Susceptibility of p21Waf1/Cip1-deficient Mice. *Cancer Res* **2001**;61:6234-8.

63.   Gao X, Chen YQ, Wu N, Grignon DJ, Sakr W, Porter AT*, et al.* Somatic mutations of the WAF1/CIP1 gene in primary prostate cancer. *Oncogene* **1995**;11:1395-8.

64.   Furutani M, Arii S, Tanaka H, Mise M, Niwano M, Harada T*, et al.* Decreased expression and rare somatic mutation of the CIPl/WAFl gene in human hepatocellular carcinoma. *Cancer Lett* **1997**;111:191-7.

65.   Klein U, Lia M, Crespo M, Siegel R, Shen Q, Mo T*, et al.* The DLEU2/miR-15a/16-1 cluster controls B cell proliferation and its deletion leads to chronic lymphocytic leukemia. *Cancer Cell* **2010**;17:28-40.

66.   Lia M, Carette A, Tang H, Shen Q, Mo T, Bhagat G*, et al.* Functional dissection of the chromosome 13q14 tumor-suppressor locus using transgenic mouse lines. *Blood* **2012**;119:2981-90.

67.   Yie Liu MC, Rasool O, Ivanova G, Ibbotson R, Grander D, Iyengar A*, et al.* Cloning of two candidate tumor suppressor genes within a 10 kb region on chromosome 13q14, frequently deleted in chronic lymphocytic leukemia. *Oncogene* **1997**;15:2463-73.

68.   Shen H, Powers N, Saini N, Comstock CE, Sharma A, Weaver K*, et al.* The SWI/SNF ATPase Brm is a gatekeeper of proliferative control in prostate cancer. *Cancer Res* **2008**;68:10154-62.

69.   Gunduz E, Gunduz M, Ali MA, Beder L, Tamamura R, Katase N*, et al.* Loss of heterozygosity at the 9p21-24 region and identification of BRM as a candidate tumor suppressor gene in head and neck squamous cell carcinoma. *Cancer Invest* **2009**;27:661-8.

70.   Endo M, Yasui K, Zen Y, Gen Y, Zen K, Tsuji K*, et al.* Alterations of the SWI/SNF chromatin remodelling subunit-BRG1 and BRM in hepatocellular carcinoma. *Liver Int* **2013**;33:105-17.

71.   Oike T, Ogiwara H, Nakano T, Yokota J, Kohno T. Inactivating mutations in SWI/SNF chromatin remodeling genes in human cancer. *Jpn J Clin Oncol* **2013**;43:849-55.

72.   Podsypanina K, Ellenson LH, Nemes A, Gu JG, Tamura M, Yamada KM*, et al.* Mutation of Pten/Mmac1 in mice causes neoplasia in multiple organ systems. *Proc Natl Acad Sci U S A* **1999**;96:1563-8.

73.   Cristofano AD, Pesce B, Cordon-Cardo C, Pandolfi PP. Pten is essential for embryonic development and tumour suppression. *Nature genetics* **1998**;19:348-55.

74.   Liaw D, March D, Li J, Dahia P, Wang S, Zheng Z*, et al.* Germline mutations of the PTEN gene in Cowden disease, an inherited breast and thyroid cancer syndrome. *Nature genetics* **1997**;16:64-7.

75.   Steck PA, Pershouse MA, Jasser SA, Yung WKA, Lin H, Ligon AH*, et al.* Identification of a candidate tumour suppressor gene, MMAC1, at chromosome 10q23.3 that is mutated in multiple advanced cancers. *Nature Genetics* **1997**;15:356-62.

76.   Li J, Yen C, Liaw D, Podsypanina K, Bose S, Wang SI*, et al.* PTEN, a putative protein tyrosine phosphatase gene mutated in human brain, breast, and prostate cancer. *Science* **1997**;275:1943-7.

77.   Neumann M, Seehawer M, Schlee C, Vosberg S, Heesch S, von der Heide EK*, et al.* FAT1 expression and mutations in adult acute lymphoblastic leukemia. *Blood Cancer J* **2014**;4:e224.

78.   Morris LG, Kaufman AM, Gong Y, Ramaswami D, Walsh LA, Turcan S*, et al.* Recurrent somatic mutation of FAT1 in multiple human cancers leads to aberrant Wnt activation. *Nat Genet* **2013**;45:253-61.

79.   van Haaften G, Dalgliesh GL, Davies H, Chen L, Bignell G, Greenman C*, et al.* Somatic mutations of the histone H3K27 demethylase gene UTX in human cancer. *Nat Genet* **2009**;41:521-3.

80.   Jankowska AM, Makishima H, Tiu RV, Szpurka H, Huang Y, Traina F*, et al.* Mutational spectrum analysis of chronic myelomonocytic leukemia includes genes associated with epigenetic regulation: UTX, EZH2, and DNMT3A. *Blood* **2011**;118:3932-41.

81.   Bailey P, Chang DK, Nones K, Johns AL, Patch AM, Gingras MC*, et al.* Genomic analyses identify molecular subtypes of pancreatic cancer. *Nature* **2016**;531:47-52.

82.   Okada N, Lin CP, Ribeiro MC, Biton A, Lai G, He X*, et al.* A positive feedback between p53 and miR-34 miRNAs mediates tumor suppression. *Genes Dev* **2014**;28:438-50.

83. Cheng CY, Hwang CI, Corney DC, Flesken-Nikitin A, Jiang L, Oner GM, *et al.* miR-34 cooperates with p53 in suppression of prostate cancer by joint regulation of stem cell compartment. *Cell Rep* **2014**;6:1000-7.

84. Welch C, Chen Y, Stallings RL. MicroRNA-34a functions as a potential tumor suppressor by inducing apoptosis in neuroblastoma cells. *Oncogene* **2007**;26:5017-22.

85. Yin D, Ogawa S, Kawamata N, Leiter A, Ham M, Li D, *et al.* miR-34a functions as a tumor suppressor modulating EGFR in glioblastoma multiforme. *Oncogene* **2013**;32:1155-63.

86. Finnberg N, Klein-Szanto AJ, El-Deiry WS. TRAIL-R deficiency in mice promotes susceptibility to chronic inflammation and tumorigenesis. *J Clin Invest* **2008**;118:111-23.

87. Lee SH, Shin MS, Kim HS, Lee HK, Park WS, Kim SY, *et al.* Alterations of the DR5/TRAIL receptor 2 gene in non-small cell lung cancers. *Cancer Res* **1999**;59:5683-6.

88. Lee SH, Shin MS, Kim HS, Lee HK, Park WS, Kim SY, *et al.* Somatic mutations of TRAIL-receptor 1 and TRAIL-receptor 2 genes in non-Hodgkin's lymphoma. *Oncogene* **2001**;20:399-403.

89. Shin MS, Kim HS, Lee SH, Park WS, Kim SY, Park JY, *et al.* Mutations of tumor necrosis factor-related apoptosis-inducing ligand receptor 1 (TRAIL-R1) and receptor 2 (TRAIL-R2) genes in metastatic breast cancers. *Cancer Res* **2001**;61:4942-6.

90. Nakau M, Miyoshi H, Seldin MF, Imamura M, Oshima M, Taketo MM. Hepatocellular carcinoma caused by loss of heterozygosity in Lkb1 gene knockout mice. *Cancer Res* **2002**;62:4549-53.

91. Miyoshi H, Nakau M, Ishikawa TO, Seldin MF, Oshima M, Taketo MM. Gastrointestinal hamartomatous polyposis in Lkb1 heterozygous knockout mice. *Cancer Res* **2002**;62:2261-6.

92. Hemminki A, Markie D, Tomlinson I, Avizienyte E, Roth S, Loukola A, *et al.* A serine/threonine kinase gene defective in Putz-Jeghers syndrome. *Letters to Nature* **1998**;391:184-7.

93. Avizienyte E, Loukola A, Roth S, Hemminki A, Tarkkanen M, Salovaara R, *et al.* LKB1 somatic mutations in sporadic tumors. *Am J Pathol* **1999**;154:677-81.

94.   Bignell GR, Barfoot R, Seal S, Collins N, Warren W, Stratton MR. Low frequency of somatic mutations in the LKB1/Peutz-Jeghers syndrome gene in sporadic breast cancer. *Cancer Res* **1998**;58:1384-6.

95.   Avizienyte E, Roth S, Loukola A, Hemminki A, Lothe RA, Stenwig AE*, et al.* Somatic mutations in LKB1 are rare in sporadic colorectal and testicular tumors. *Cancer Res* **1998**;58:2087-90.

96.   Ohki R, Saito K, Chen Y, Kawase T, Hiraoka N, Saigawa R*, et al.* PHLDA3 is a novel tumor suppressor of pancreatic neuroendocrine tumors. *Proc Natl Acad Sci U S A* **2014**;111:E2404-13.

97.   Hu Q, Gao F, Tian W, Ruteshouser EC, Wang Y, Lazar A*, et al.* Wt1 ablation and Igf2 upregulation in mice result in Wilms tumors with elevated ERK1/2 phosphorylation. *J Clin Invest* **2011**;121:174-83.

98.   Haber DA, Housman DE. Role of the Wt1 Gene in Wilms-Tumor. *Cancer Surveys* **1992**;12:105-17.

99.   Chen X, Yang Y, Huang Y, Tan J, Chen Y, Yang J*, et al.* WT1 mutations and single nucleotide polymorphism rs16754 analysis of patients with pediatric acute myeloid leukemia in a Chinese population. *Leuk Lymphoma* **2012**;53:2195-204.

100.   Coppes MJ, Liefers GJ, Paul P, Yeger H, Williams BR. Homozygous somatic Wt1 point mutations in sporadic unilateral Wilms tumor. *Proc Natl Acad Sci U S A* **1993**;90:1416-9.

101.   Paik JH, Kollipara R, Chu G, Ji H, Xiao Y, Ding Z*, et al.* FoxOs are lineage-restricted redundant tumor suppressors and regulate endothelial cell homeostasis. *Cell* **2007**;128:309-23.

102.   Trinh DL, Scott DW, Morin RD, Mendez-Lago M, An J, Jones SJ*, et al.* Analysis of FOXO1 mutations in diffuse large B-cell lymphoma. *Blood* **2013**;121:3666-74.

103.   Mercado GE, Barr FG. Fusions Involving PAX and FOX Genes in the Molecular Pathogenesis of Alveolar Rhabdomyosarcoma: Recent Advances. *Current Molecular Medicine* **2007**;7:47-61.

104.   Dong XY, Chen C, Sun X, Guo P, Vessella RL, Wang RX*, et al.* FOXO1A is a candidate for the 13q14 tumor suppressor gene inhibiting androgen receptor signaling in prostate cancer. *Cancer Res* **2006**;66:6998-7006.

105. Ming Kwan K, Li AG, Wang XJ, Wurst W, Behringer RR. Essential roles of BMPR-IA signaling in differentiation and growth of hair follicles and in skin tumorigenesis. *Genesis* **2004**;39:10-25.

106. Edson MA, Nalam RL, Clementi C, Franco HL, Demayo FJ, Lyons KM*, et al.* Granulosa cell-expressed BMPR1A and BMPR1B have unique functions in regulating fertility but act redundantly to suppress ovarian tumor development. *Mol Endocrinol* **2010**;24:1251-66.

107. Zhou XP, Woodford-Richens K, Lehtonen R, Kurose K, Aldred M, Hampel H*, et al.* Germline mutations in BMPR1A/ALK3 cause a subset of cases of juvenile polyposis syndrome and of Cowden and Bannayan-Riley-Ruvalcaba syndromes. *Am J Hum Genet* **2001**;69:704-11.

108. Howe JR, Sayed MG, Ahmed AF, Ringold J, Larsen-Haidle J, Merg A*, et al.* The prevalence of MADH4 and BMPR1A mutations in juvenile polyposis and absence of BMPR2, BMPR1B, and ACVR1 mutations. *J Med Genet* **2004**;41:484-91.

109. Karoui M, Tresallet C, Julie C, Zimmermann U, Staroz F, Brams A*, et al.* Loss of heterozygosity on 10q and mutational status of PTEN and BMPR1A in colorectal primary tumours and metastases. *Br J Cancer* **2004**;90:1230-4.

110. El-Deiry WS, Tokino T, Velculescu VE, Levy DB, Parsons R, Trent JM*, et al.* WAF1, a Potential Mediator of p53 Tumor Suppression. *Cell* **1993**;75:817-25.

111. Liu X, Ory V, Chapman S, Yuan H, Albanese C, Kallakury B*, et al.* ROCK inhibitor and feeder cells induce the conditional reprogramming of epithelial cells. *Am J Pathol* **2012**;180:599-607.

112. Baker SJ, Markowitz S, Fearson ER, Wilson JKV, Vogelstein B. Suppression of Human Colorectal Carcinoma Cell Growth by Wild-Type p53. *Science* **1990**;249:912-5.

113. Resnick-Silverman L, Clair SS, Maurer M, Kathy Zhao, Manfredi JJ. Identification of a novel class of genomic DNA binding sites suggests a mechanism for selectivity in target gene activation by the tumor suppressor protein p53. *Genes & Development* **1998**;12:2102-7.

114. Lois C, Hong EJ, Shirley Pease, Brown EJ, Baltimore D. Germline Transmission and Tissue-Specific Expression of Transgenes Delivered by Lentiviral Vectors. *Science* **2002**;295:868-72.

115. Blanchette M, Kent WJ, Riemer C, Elnitski L, Smit AFA, Roskin KM*, et al.* Aligning Multiple Genomic Sequences With the Threaded Blockset Aligner. *Genome Res* **2004**:708-15.

116. Heinz S, Benner C, Spann N, Bertolino E, Lin YC, Laslo P*, et al.* Simple combinations of lineage-determining transcription factors prime cis-regulatory elements required for macrophage and B cell identities. *Mol Cell* **2010**;38:576-89.

117. Ernst J, Kellis M. Discovery and characterization of chromatin states for systematic annotation of the human genome. *Nature biotechnology* **2010**;28:817-25.

118. Wasserman WW, Sandelin A. Applied bioinformatics for the identification of regulatory elements. *Nat Rev Genet* **2004**;5:276-87.

119. Futreal PA, Coin L, Marshall M, Down T, Hubbard T, Wooster R*, et al.* A census of human cancer genes. *Nat Rev Cancer* **2004**;4:177-83.

120. Subramanian A, Tamayo P, Mootha VK, Mukherjee S, Ebert BL, Gillette MA*, et al.* Gene set enrichment analysis: a knowledge-based approach for interpreting genome-wide expression profiles. *Proc Natl Acad Sci U S A* **2005**;102:15545-50.

121. Robinson JT, Thorvaldsdottir H, Winckler W, Guttman M, Lander ES, Getz G*, et al.* Integrative genomics viewer. *Nature biotechnology* **2011**;29:24-6.

122. Thorvaldsdottir H, Robinson JT, Mesirov JP. Integrative Genomics Viewer (IGV): high-performance genomics data visualization and exploration. *Brief Bioinform* **2013**;14:178-92.